Collapse load evaluation of pinned-joint composite plates

Aurora Pisano, Paolo Fuschi

DASTEC, University Mediterranea of Reggio Calabria, Italy
E-mail: *aurora.pisano@unirc.it, paolo.fuschi@unirc.it*

Keywords: Limit Analysis Theory, Linear Matching Method, Mechanically-Fastened Composite Joints.

SUMMARY. A numerical procedure for limit analysis is presented and applied to evaluate upper and lower bounds to the collapse load of pinned-joint composite plates. The procedure is an extension, in the context of orthotropic materials, of a method known in the literature as Linear Matching Method. To show the validity of the method, the numerical predictions are compared with available experimental data in terms either of collapse loads or of collapse mechanisms.

1 INTRODUCTION

Joints between composite laminates, among several techniques, can be made by using mechanical fasteners like bolts, rivets or pin-connectors. Mechanical fastened-joints are employed in many advanced engineering fields and this mainly because they are relatively inexpensive to manufacture as well as easy to assemble or disassemble. Nevertheless, such type of connections are characterized by an high stress concentration near the hole area which becomes a source of weakness; the structural joint failure usually begins at the fasteners sites. A great deal of research has therefore concentrated on the evaluation of the strength as well as on the prediction of the failure mechanism of these joints between composite plates or components and this with different approaches, see e.g. [1] and references therein.

In the present study, far off the will of furnishing an exhaustive solution of the above problem, a *limit analysis numerical approach* for pinned-joint orthotropic composite laminates in plane stress conditions is proposed. The mechanical problem is treated in terms of evaluation of an upper and a lower bound to the collapse load multiplier giving also a prediction of the failure mode. The examined structural elements are composite laminates obeying, by hypothesis, to a Tsai-Wu type yield criterion defined as a second order tensor polynomial form of the Tsai-Wu failure criterion for composite laminates [2]. This criterion is one of the best known showing a very good capability for predicting the failure of composite laminates [3].

The treated numerical approach, recently proposed by the authors in [4,5], can be viewed as an extension, in the context of orthotropic materials, of a method known in the relevant literature as *Linear Matching Method* (LMM), see e.g. [6]. The LMM here employed basically solves a sequence of linear analyses on the structure assumed, by hypothesis, as made of a *fictitious linear viscous orthotropic material* with *spatially varying moduli* and suffering a distribution of *given initial stresses*. With this conjecture, at each iteration, by varying (rescaling) the fictitious material parameters at each sampling point of the structure (namely at each Gauss point of the adopted FE mesh), the computed fictitious solution is used to define a collapse mechanism for the real structure and eventually an upper bound to the collapse load multiplier. The whole method has

been rephrased in a dimensionless stress space turning to an iterative procedure easy to handle, the number of fictitious material parameters to be adjusted reducing drastically to a scalar one. The proposed approach provides also a pseudo lower bound to the collapse load. At each iteration of the above summarized procedure the maximum computed stress is appropriately rescaled in order to satisfy the admissibility conditions. Applying the rescaling factor to all the other stress values, a statically admissible stress distribution can be computed. The latter, following the static approach of limit analysis, is used to evaluate a lower bound to the collapse load. In practice the obtained lower bound is a lower bound to the least upper bound of the computed sequence. Such evaluation appears to be very useful for design purposes being able to predict a range of limit load values within which the collapse load should be located.

Few numerical examples are carried out to verify the effectiveness of the proposed approach as well as to inquire into its capability to predict experimental test results for pinned-joint composite prototypes. The obtained results are compared with experimental laboratory tests traceable in the relevant literature, [7]. The results, obtained in terms of collapse mode prediction of the analyzed prototypes, are indeed very encouraging either for the good agreement with the experimental findings or for the ability of the proposed procedure to locate accurately the collapse zone and the related collapse mode.

2 THE MECHANICAL PROBLEM

The mechanical problem under study concerns a pinned-joint rectangular composite plate in tension, like the one schematically represented in Figure 1, where geometrical and loading quantities are also reported. The plate is subjected to a uniform tensile load distribution acting on the plate plane and equivalent to a load P. The load is transmitted via the fastener to the plate in a way that is very difficult to exactly determine, however, research studies [8] have demonstrate that, inside the hole, an approximation of the actual loading condition is given by a cosine pressure distribution.

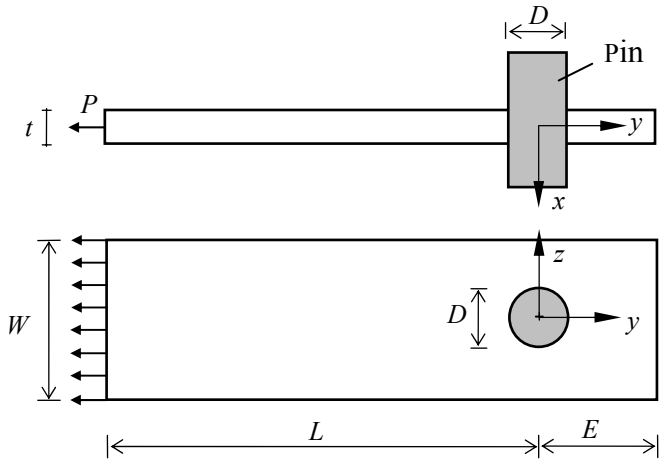

Figure 1: Schematic representation of a pin-loaded plate.

As pointed out in the relevant literature [9], the failure of a mechanical fastened joint depends on its geometry, fiber orientation, position of the hole, besides the environmental conditions

affecting the mechanical properties of the material. A lot of experimental work has then been carried out to correlate the effects of geometric parameters (width-diameter ratio W/D, edge distance-diameter ratio E/D) as well as the effects of the aged material on the bearing strength and failure modes of the joint [10-11]. Typically, three fundamental modes of failure can be individuated, other modes being a combination of them; Figure 2 sketches the three basic failure modes commonly used in the literature. Precisely, the *tension-net* failure mode which is due to high tensile stress value on the net area through the fastener hole; the *shear-out* failure mode which is related to the transverse failure of the material and, finally, the *bearing* failure mode characterized by high compressive stress values within the zone surrounding the loaded inner surface. The first two modes are usually catastrophic, while the latest is a progressive failure mode.

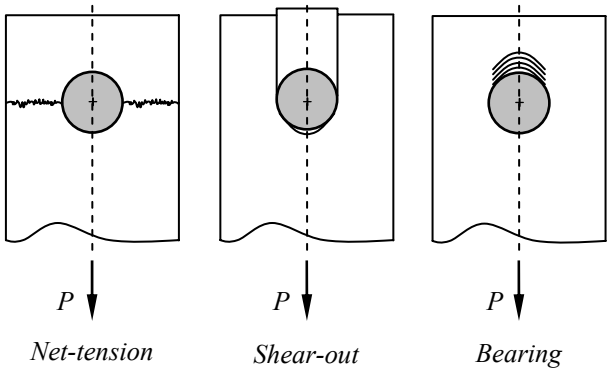

Figure 2: Illustration of the three basic failure modes reported in the literature.

It appears then evident that, for the studied problem, the prediction of the collapse load as well as of the collapse mechanism is a crucial goal and this justifies the researchers' interest in developing analytical and/or numerical procedures to solve the problem. In the present context, such problem is treated on the base of the following (simplifying) assumptions:

- three dimensional effects are neglected and a stress-plane problem is considered;
- the effects of the actual stacking sequence of the laminate are assumed not critical and an equivalent single layer laminate is analyzed;
- renouncing to the description of the complex stress state arising within the joint, the evaluation of the load bearing capacity is pursued by means of a limit analysis approach. To this aim the LMM is applied for the evaluation of an upper and a lower bound to the collapse load multiplier.

The fundamentals of the LMM, which has been extended by the authors to the case of orthotropic material in [4] and recently systematized and improved in [5], are briefly summarized in the next section.

3 UPPER AND LOWER BOUNDS TO THE COLLAPSE LOAD *VIA* LMM

Following a standard formalism of the kinematic approach of limit analysis theory, an upper bound to the collapse limit load multiplier, for a given body of volume V, is given by:

$$P_{UB}\int_{\partial V_t}\overline{p}_i\dot{u}_i^c\,\mathrm{d}\partial V=\int_V\sigma_j^y\dot{\varepsilon}_j^c\,\mathrm{d}V, \tag{1}$$

where $\dot{\varepsilon}_j^c=\dot{\lambda}\,\partial f/\partial\sigma_j$ are the components of the outward normal to the yield surface $f(\sigma_j)=0$ (with $\dot{\lambda}>0$ a positive scalar multiplier); σ_j^y are the stresses at yield associated to given compatible strain rates $\dot{\varepsilon}_j^c$; $\dot{u}_i^c$ are the related displacement rates. $\overline{p}_i$ are the surface force components of the reference load vector $\overline{\boldsymbol{p}}$ acting on the external portion ∂V_t of the body surface. Finally, P_{UB} denotes the upper bound load multiplier. The set ($\dot{\varepsilon}_j^c$, $\dot{u}_i^c$) defines a collapse mechanism. On the other hand, if at every point within V exists a stress field, say $\tilde{\sigma}_j$, which satisfies the condition $f(\tilde{\sigma}_j)\le 0$ and in equilibrium with the applied load $P\,\overline{\boldsymbol{p}}$ for a value of P, say P_{LB}, then P_{LB} is a lower bound on the collapse limit load multiplier.

The proposed numerical procedures is aimed to individuate the kinematic quantities $\dot{\varepsilon}_j^c,\dot{u}_i^c$ for the evaluation of a P_{UB} or, alternatively, to define an equilibrated stress distribution, satisfying the admissibility condition, for the evaluation of the P_{LB}. As already declared in the introductory section, the LMM is an iterative numerical procedure involving a sequence of FE-based analyses carried out on the structure under study assuming it as made of a fictitious material with spatially varying elastic moduli. In particular, at each iteration the fictitious moduli are adjusted so that the computed fictitious stresses are brought on the yield surface at a fixed strain rate distribution. This allows one to define a collapse mechanism ($\dot{\varepsilon}_j^c,\dot{u}_i^c$), the related stress at yield σ_j^y and then, by means of eq.(1) a P_{UB} load multiplier. From the geometrical point of view, the procedure simply states that the complementary energy equipotential surface of the fictitious elastic material, say $W(\sigma_j)=const$, must be brought to be tangential to (i.e. to match) the yield surface at the stress point $\boldsymbol{\sigma}^y$ whose external normal is $\dot{\boldsymbol{\varepsilon}}^c$.

In the case of orthotropic materials, the LMM utilizes two fundamental assumptions:

- the fictitious material, the structure is made with, is an orthotropic linear viscous material subjected to a distribution of imposed initial stresses;
- the considered material obeys, by hypothesis, to a simplified second order form of the Tsai-Wu constitutive relation.

As consequence of the first assumption, taking advantage from the formal analogy between the linear viscous and the linear elastic problem, a fictitious linear elastic solution can be computed as a fictitious elastic solution having the same complementary energy potential functional $W(\sigma_j)$. The numerical analysis involved in the iterative procedure can then be carried out by any commercial FE code with obvious advantages.

For what concerns the second assumption, it is worth to remind that, in a dimensionless stress space, the simplified second order form of the Tsai-Wu criterion can be written as:

$$X^2+Y^2+Z^2+2f_{12}XY+f_1X+f_2Y=1, \tag{2}$$

where f_1,f_2,f_{12} are constant coefficients related to the strength parameters of the material. Eq.(2) individuates, in the dimensionless space (X, Y, Z), an ellipsoid whose major axis lies on the $Z = 0$ plane. This circumstance, using the geometrical interpretation of the linear matching method, above reminded, allows to simplify the procedure. As in fact, for each iteration (since the beginning), it is possible to define the fictitious material in such a way that its complementary energy equipotential surface is an ellipsoid homothetic to the Tsai-Wu one so that, at matching, the two ellipsoids become coincident. As a consequence, only one scalar parameter has to be iteratively updated, namely the *homothetic ratio* between the two ellipsoids, parameter which is

directly related to the fictitious elastic moduli of the material.

3.1 *Iterative scheme of the LMM for the upper and lower bounds evaluation*

In the following, for brevity, a flow-chart version of the whole procedure is reported, while for more details the reader can referee to [5].

Initialization

Knowing the strength values of the orthotropic material (X_c; X_t; Y_c; Y_t; S), assign to all FEs in the mesh an initial set of fictitious elastic parameters and initial stresses such that the complementary energy equipotential surface is homothetic to the Tsai-Wu surface, i.e.:

$$E_1^{(0)} = 1/(2F_{11})\,;\; E_2^{(0)} = 1/(2F_{22})\,;\quad E_6^{(0)} = 1/(2F_{66})\,;\quad \nu_{12}^{(0)} = -f_{12}\sqrt{F_{11}}/\sqrt{F_{22}}\,;$$

$$\overline{\sigma}_1^{(0)} = \alpha_{TW}/\sqrt{F_{11}}\,;\; \overline{\sigma}_2^{(0)} = \beta_{TW}/\sqrt{F_{22}}\,;\; \overline{\sigma}_6^{(0)} = 0\,,$$

α_{TW} and β_{TW} being the X, Y coordinates of the Tsai-Wu ellipsoid centre, while F_{11}, F_{22} and F_{66} are functions of the strength values [9].

Set also: k = 1, $P_{UB}^{(k-1)} = P_{UB}^{(0)} = 1$ (for k = 1, $P_{UB}^{(0)}$ can be any arbitrary value) and compute the constant quantity $\Omega = 1 + \alpha_{TW}^2 + 2f_{12}\alpha_{TW}\beta_{TW} + \beta_{TW}^2$ for later use.

Iteration loop

step #1 perform a fictitious elastic analysis with elastic parameters $E_j^{(k-1)}$, $\nu_{12}=\nu_{12}^{(0)}$, initial stresses $\overline{\sigma}_j = \overline{\sigma}_j^{(0)}$ and with loads $P_{UB}^{(k-1)}\overline{p}_i$, computing a fictitious elastic solution, at Gauss point (GP) level, namely: $\dot{\varepsilon}_j^{e(k-1)}$, $\dot{u}_j^{(k-1)}$, $\sigma_j^{e(k-1)}$.

step #2 compute the constant value of the complementary potential energy:

$$\overline{W}^{(k-1)} = \frac{1}{2}\sigma_j^{e(k-1)}\varepsilon_j^{e(k-1)}\,.$$

step #3 compute the homothety ratio, namely

$$\Gamma^{(k-1)} = \begin{cases} \sqrt{\Omega/\overline{W}^{(0)}} & \text{for} \quad k = 1 \\ \sqrt{\overline{W}^{(k-2)}/\overline{W}^{(k-1)}} & \text{for} \quad k > 1 \end{cases}$$

step #4 evaluate stresses at yield:

$$\sigma_1^{y(k-1)} = \left[1-\Gamma^{(k-1)}\right]\frac{\alpha_{TW}}{\sqrt{F_{11}}} + \Gamma^{(k-1)}\sigma_1^{e(k-1)}\,;$$

$$\sigma_2^{y(k-1)} = \left[1-\Gamma^{(k-1)}\right]\frac{\beta_{TW}}{\sqrt{F_{22}}} + \Gamma^{(k-1)}\sigma_2^{e(k-1)}\,;$$

$$\sigma_6^{y(k-1)} = \Gamma^{(k-1)}\sigma_6^{e(k-1)}\,.$$

step #5 set $\dot{\varepsilon}_j^{c(k-1)} = \dot{\varepsilon}_j^{e(k-1)}$, $\dot{u}_i^{c(k-1)} = \dot{u}_i^{e(k-1)}$ and evaluate the upper bound multiplier

$$P_{UB}^{(k)} = \frac{\int_V \sigma_j^{y(k-1)}\dot{\varepsilon}_j^{c(k-1)}\mathrm{d}V}{\int_{\partial V_t}\overline{p}_i\dot{u}_i^{c(k-1)}\mathrm{d}\partial V}\,.$$

step #6 evaluate a lower bound multiplier $P_{LB}^{(k)} := \rho^{(k)}P_{UB}^{(k)}$, where $\rho^{(k)}$ is a rescaling factor of the applied load so that all the fictitious elastic stresses $\rho^{(k)}\,\boldsymbol{\sigma}^{e(k)}$ satisfy the condition $f \le 0$.

step #7 check for convergence

$$\left|P_{UB}^{(k)} - P_{UB}^{(k-1)}\right| \le \text{Toll} \quad \begin{cases} Yes \Rightarrow Exit \\ Not \Rightarrow Continue \end{cases}$$

step #8 compute the $E_j^{(k)}$ distribution accomplishing the matching at each GP, to be utilized, if necessary, at next iteration, namely:

$$E_j^{(k)} = E_j^{(k-1)} \left[\Gamma^{(k-1)}\right]^2, \quad j = 1,2,6$$

set $k = k - 1$ and go to step #1.

With reference to the above procedure, the evaluation of the lower bound collapse multiplier, P_{LB}, requires some more comments. At each iteration and at each GP, the fictitious dimensionless stresses $\boldsymbol{\chi}^{e(k)}$ pertinent to loads $P_{UB}^{(k)}\ \bar{\boldsymbol{p}}$ and Young moduli distribution $E_j^{(k)}$, are located in the (*X, Y, Z*) space; see also the schematic sketch given in Figure 3 for three generic GPs in the Z = 0 plane.

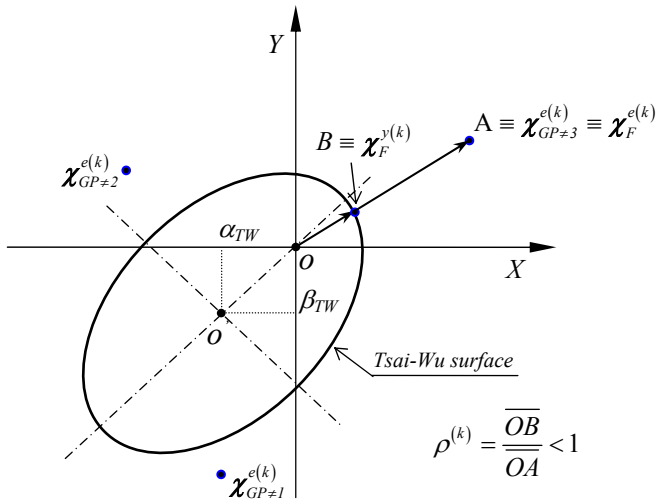

Figure 3: Evaluation of the factor $\rho^{(k)}$ for the $P_{LB}^{(k)}$ evaluation.

Among all the stress points $\boldsymbol{\chi}^{e(k)}$ obtained the one further away from the Tsai Wu surface is detected, $\boldsymbol{\chi}_F^{e(k)}$ (point A in Figure 3), and this merely by computing the Euclidean distances from the Tsai Wu ellipsoid centre. The ratio $\rho^{(k)}$ between the yield stress value measured on the direction $\boldsymbol{\chi}_F^{e(k)} / \left|\boldsymbol{\chi}_F^{e(k)}\right|$, say $\boldsymbol{\chi}_F^{y(k)}$ (point B in Figure 3), over the stress value $\boldsymbol{\chi}_F^{e(k)}$ allows one to define the lower bound defined in step#6. The P_{LB}, as evaluated above, appears to be too conservative because it depends on only one stress value attained at one GP in the whole mesh (the one further away from the Tsai Wu surface). On taking into account that the static approach of limit analysis essentially states that the structure rearranges the internal stresses to its best possible advantage to withstand the applied loads, the stress values measured at the GPs of the FEs can be averaged to within each element. With this averaged stress values can then be evaluated an averaged $\rho^{(k)}$, say $\bar{\rho}^{(k)}$. A weighted lower bound, say P_{WLB}, is then computed (at step #6),

namely: $P_{WLB}^{(k)} := \overline{\rho}^{(k)} P_{UB}^{(k)}$. The latter definition of the P_{LB} is the one used in the in the following numerical applications.

4 NUMERICAL APPLICATIONS AND REMARKS

The LMM is applied to the mechanical problem described in Section 2 and with reference to the data available in [7] where several experimental results are reported for a pin-loaded plate, in plane stress conditions. Due to the symmetry of the problem with respect to the longitudinal y axis, only one half of the plate has been analyzed, as shown in Figure 4, which also contains the material characteristics of the plate in terms of strength values and elastic moduli, the Poisson ratio is assumed equal to 0.3.

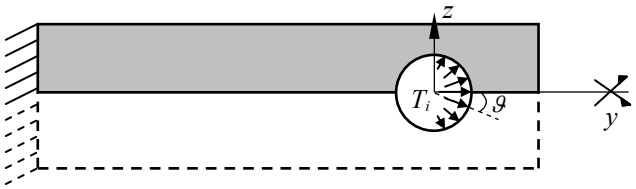

Elastic Moduli (GPa)	*Strength* (MPa)
$E_1 = 49.8$	$Y_t = X_t = 664.3$
$E_2 = 6.9$	$Y_c = X_c = 385.1$
$G_{12} = 31.9$	$S = 64.6$

Figure 4. Pin loaded plate: geometrical model and material properties.

To simulate the action of the pin inside the hole a cosine load normal distribution T_i was assumed in the form:

$$T_i = -\frac{4P}{\pi D} n_i \cos\vartheta \,, \tag{3}$$

where P is the applied load, D the diameter of the hole, n_i the unit vector normal to the inner hole surface and ϑ a clockwise angle varying in the range $[-\pi/2, \pi/2]$. The applied reference load P has been assumed equal to 1kN. All the elastic analyses have been carried out by means of the code ADINA [13], using a FE mesh of the type shown in Figure 5, with a number of elements variable depending on the geometry of the plate, and involving isoparametric shell elements with 16 nodes and 16 GPs per element. A Fortran main program has been developed to control the iterative procedure and the matching at each Gauss point as described in Section 3.1.

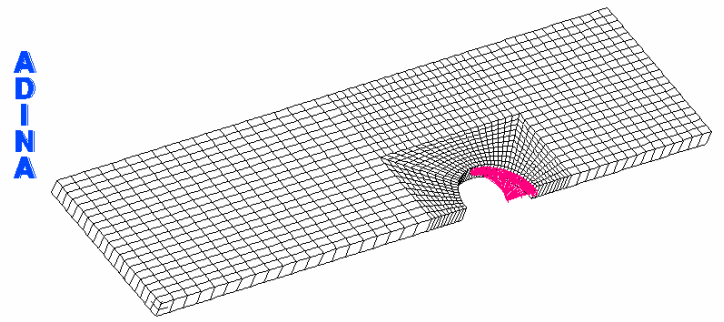

Figure 5. Pin-loaded plate: half plate FE mesh adopted.

In all the examined cases the procedure has shown a very rapid convergence, the latter assured by a sufficient condition for convergence satisfied by the present approach. For sake of brevity

only two of the computed upper and lower bound sequences are reported in Figure 6(a,b). Indeed, many of the experimental tests reported in [7] have been numerically reproduced and the obtained results are reported in Table 1 for sake of comparison. The latter is made in terms of ultimate bearing strength, namely σ_{BRU}, defined as the *"maximum stress reached before a reduction in stress occurs for the first time"*. This bearing strength is given by the ratio between the load at failure, say P_F , and the product of the hole diameter times the plate thickness: $\sigma_{BRU} := P_F /Dt$. Table 1 reports, for 16 specimens: the geometry; the experimental values of σ_{BRU} together with the experimentally observed failure mechanisms; the predicted σ_{BRU} given by the present analysis. In particular, the σ_{BRU} values given by the present LMM, namely the upper and the lower σ_{BRU}, have been computed at last iteration as: $\sigma_{BRU} = P_{UB}P/Dt$ and $\sigma_{BRU} = P_{WLB}P/Dt$.

Table 1. Pin-loaded plate of Figure 4: experimental bearing strength values and failure modes against predicted bearing strengths

Specimen dimensions					*Experimental**		*Prediction by LMM*	
Item Number	*D* (*mm*)	*W/D*	*E/D*	*t* (*mm*)	σ_{BRU} (MPa)	Failure mode	*Upper* σ_{BRU} (MPa)	*Lower* σ_{BRU} (MPa)
1	6.35	4	3	1.24	329	T	386	327
2	6.35	4	3	2.48	537	T	386	327
3	6.35	4	3	5.63	613	T	386	327
4	6.35	8	3	1.15	421	B/S	387	325
5	6.35	8	3	2.41	499	B	387	325
6	6.35	8	3	5.62	611	B	387	325
7	6.35	4	2	2.33	460	T	255	210
8	6.35	4	4	2.31	491	B/T	513	397
9	6.35	4	6	2.32	496	T	520	387
10	6.35	8	2	2.31	458	S	255	238
11	6.35	8	4	2.27	522	B/S	518	443
12	6.35	8	6	2.28	439	B	532	516
13	12.70	4	3	1.15	281	B	385	362
14	12.70	4	3	2.41	376	B	385	362
15	12.70	4	3	5.63	486	B/T	385	362
16	12.70	4	3	12.71	564	T	385	362

* after Wu & Hahn 1998 [7].

By examining the results of Table 1, it can be noted that the differences on the σ_{BRU} values are, in several cases, very high. To this concern, sharing the convincement of the above quoted paper, these discrepancies could be caused by a three dimensional effect which is not considered with a 2D FE formulation. Indeed, the same values of σ_{BRU} obtained for prototypes having the same *W/D* and *E/D* ratios but with different thickness are consistent with the 2D FE analysis but contradict the experimental evidences. To this concern it is to observe that a different thickness implies a different stacking sequence of the laminate layers that can strongly affect the mechanical

characteristics of the laminate. Other results, about half of the run examples, are very good with a low error in percentage, but the above drawbacks need further investigations.

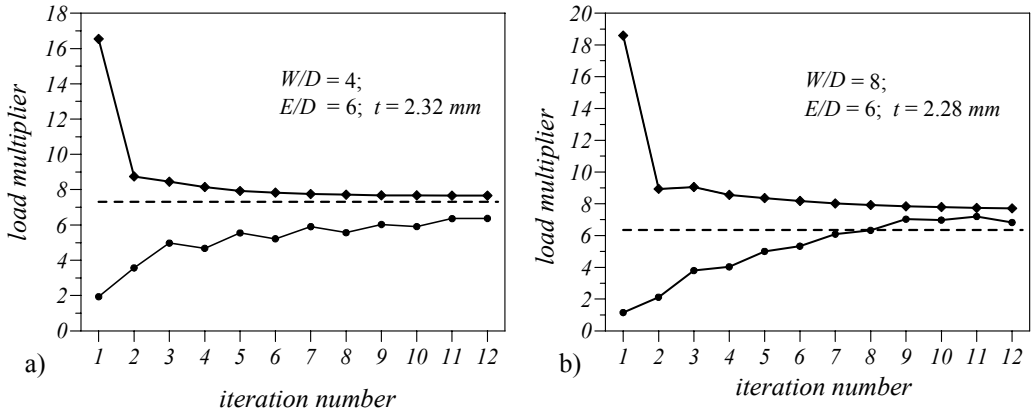

Figure 6. Upper bound (solid line with diamonds), lower bound (solid line with circles) and experimental load multiplier (dashed line) versus iteration numbers for: a) item #9, b) item #12.

It is worth to note that the procedure allows also to individuate the collapse mechanism by the band plots, at last iteration, of the node displacement components. With reference to the case a) of Figure 6, namely for specimen #9, the collapse mechanism is plotted in Figures 7 in which a net-tension failure mode can evidently be recognized. The same failure mode have been observed experimentally for the considered specimen. A very good prediction of the collapse mechanism has been found in almost all the examined cases here not reported for brevity. These results are obvious very promising, either for the good agreement with the experimental findings or for the precise definition of the collapse zone, but the proposed analysis needs definitively further improvements.

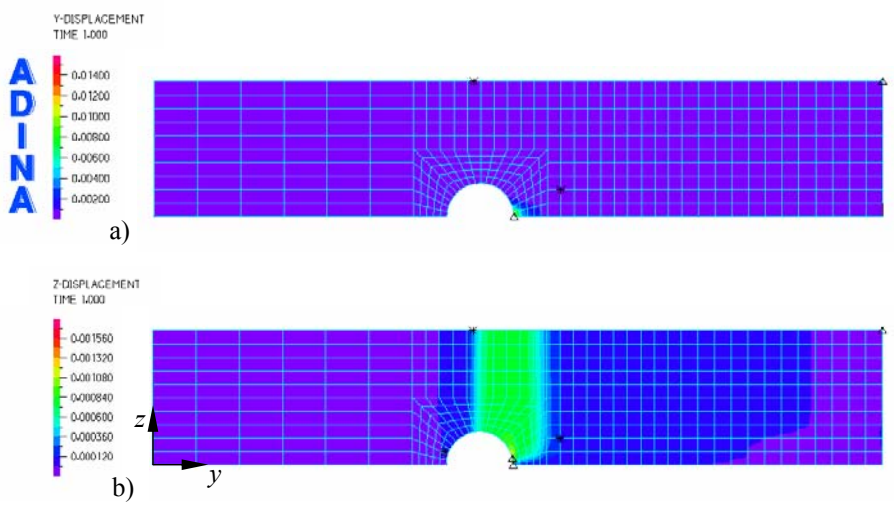

Figure 7. Pin-loaded plate of Figure 4, collapse mechanism of net- tension type for specimen #9: a) *y*-displacements; b) *z*-displacements.

References

[1] H. A. Whitworth, O. Aluko, N. A. Tomlinson. "Application of the point stress criterion to the failure of composite pinned joints". *Engineering Fracture Mechanics*, **75**, 1829-1839, (2008).

[2] S. W. Tsai, E. M. Wu. "A general theory of strength for anisotropic materials". *Jounal of Composite Materials*, **5**, 58-80, (1971).

[3] M. J. Hinton, P. D. Soden, A. S. Kaddour. "A comparison of the predicted capabilities of current failure theories for composite laminates, judged against experimental evidence". *Composites Science and Technolgy*, **62**, 1725-1797, (2002).

[4] A. A. Pisano, P. Fuschi. "A numerical approach for limit analysis of orthotropic composite laminates". *International Journal for Numerical Methods in Engineering*, **70**, 71-93, (2007).

[5] P. Fuschi, A. A. Pisano, O. Barrera. "Limit analysis of orthotropic laminates by Linear Matching Method", in D. Weichert, A.R.S. Ponter (Eds.), *Limit States of Materials and Structures- Direct Methods*, Springer, Wien, 197-220, (2009).

[6] H. F. Chen, A. R. S. Ponter, R. A. Ainsworth. "The linear matching method applied to the high temperature life integrity of structures. Part. 1. Assessment involving constant residual stress fields". *International Journal of Pressure Vessels and Piping*, **83**, 123-135, (2006).

[7] T. J. Wu, H. T. Hahn. "The bearing strength of e-glass/vinyl-ester composites fabricated by VARTM". *Composites Science and Technolgy*, **58**, 1519-1529, (1998).

[8] F. K. Chang. "The Effect of Pin Load Distribution on the Strength of Pin Loaded Holes in Laminated Composites." Journal of Composite Materials, **20**, 401-408, (1986).

[9] R. M. Jones, Mechanics of composite materials. 2nd edn., Taylor & Francis Inc., Philadelphia, PA, USA (1999).

[10] P. P. Camanho, F. L. Matthews. "Stress analysis and strength prediction of mechanically fastened joints in FRP: a review". *Composites part A*, **28A**, 529-547, (1997).

[11] S. D. Thoppul, J. Finegan, R. F. Gibson. "Mechanics of mechanically fastened joints in polymer-matrix composite structures - A review". *Composites Science and Technolgy*, **69**, 301-329, (2009).

[12] A. R. S. Ponter, K. F. Carter. "Limit state solutions, based upon linear elastic solutions with spatially varying elastic modulus". *Computer Methods in Applied Mechanics and Engineering*, **140**, 237-258, (1997).

[13] ADINA R & D, Inc. Theory and Modeling Guide. Adina R & D, Watertown, MA, USA. (2002).